Dynamic modelling of a railway wheelset based on Kane's method

Te Wen Tu

Department of Mechanical Engineering,
Air Force Institute of Technology,
Kaohsiung 820, Taiwan
Email: tutewen@gmail.com
Email: tu123@ms17.hinet.net

Abstract: This study applies Kane's method to generate the equations of motion for a railway wheelset moving on a tangent track at a constant speed. Since the wheel and rail close contact conditions are used to obtain two nonholonomic constraint equations, the lateral vibration of the wheelset can be proven as a nonholonomic system possessing two degrees of freedom. Moreover, using Kane's approach to derive the linearised equations, we can take advantage of bypassing the full nonlinear equations and getting two equations with dynamic decoupling. When the set of equations in this work is compared with those in the literature, we found that two gyroscopic effect terms exist and yaw gravitational stiffness disappears, so that the critical speeds calculated in this work are always lower than those in the literature for the same numerical cases. At last, the contact conditions along with the creepages between wheels and rails can be directly expressed in terms of generalised speeds by using Kane's method. It shows that Kane's method focuses on motions rather than on configurations.

Keywords: Kane's method; nonholonomic system; motion constraint; dynamic decoupling; gyroscopic effect.

Reference to this paper should be made as follows: Tu, T.W. (2020) 'Dynamic modelling of a railway wheelset based on Kane's method', *Int. J. Heavy Vehicle Systems*, Vol. 27, Nos. 1/2, pp.202–226.

Biographical notes: Te Wen Tu is an Academic Staff in Air Force Institute of Technology. He received his BS and MS in the Department of Mechanical Engineering from National Cheng Kung University (NCKU), Taiwan in 1983 and 1985, respectively. Later, in April 1992, he received his PhD in the Department of Aeronautics and Astronautics from NCKU. His research interests are Kane's dynamics, analytical solutions of heat conduction, and creative mechanism design.

1 Introduction

The prevailing high-speed railway in Japan, Europe, and China has led to the problem of achieving operational safety in the high-speed condition which requires a real-time response a pressing concern for vehicle designers all around the world. It is well-known

that a rail-vehicle system is a multibody system with numerous degrees of freedom and is usually a nonholonomic system. Thus, the complicated equations of motion for dynamic analysis must be solved by computers. However, formulating equations of motion for such systems (Zhai, 2015; Shabana et al., 2007; Iwnicki, 2006; Wickens, 2003; Garg and Dukkipati, 1984) is difficult when researchers took the classical methods, such as Newton-Euler method or Lagrange method. In general, the former method requires otherwise unnecessary calculations and introduces constraint forces or connecting forces that can be subsequently cancelled in deriving equations of motion, whereas the latter one basically involves various algebraic operations and introduces Lagrange multipliers to deal with nonholonomic systems.

In multibody dynamics, many investigators are convinced that Kane's method is superior to classical ones in saving both the labour in formulating equations of motion and the computing time for computer implementation (Banerjee, 2016; Huston, 1990). In the 1950s, Kane developed an approach that reduces the formulation of the equations of motion for a complex system to a straightforward, deductive procedure without requiring strong intuitiveness (Radetsky, 1985). Kane's method (Roithmayr and Hodges, 2016) has been mostly applied in space dynamics (Kane et al., 1983) and has yielded valuable research findings:

- the velocities and angular velocities of rigid bodies are directly written in generalised speeds, increasing the sensitivity to motions;
- optional generalised speeds with high flexibility yield concise equations of motion and reduce both the computation time and the derivation labour
- the resulting first-order dynamic equations simplify the numerical analysis
- Lagrange's multipliers are not required and both holonomic and nonholonomic systems can be applied simultaneously
- linearisation equations can directly be applied to generate the design equations of a control system
- the principle of virtual work need not be applied as deriving equations of motion.

Although some specific problems might be better solved by other approaches, Kane's method is still distinctly advantageous for general complex multibody systems. As usual, Kane's method is the most systematic and efficient, not only requiring less labour but also leading to the simplest and most intuitive dynamic equations. Per our observation, no one has investigated the dynamic analysis of rail-vehicle systems via Kane's method in the literature until today. In my opinion, there are two reasons for rail-vehicle dynamicists bypassing Kane's method.

We knew that the development of railway vehicle dynamics has been undertaken for about 200 years. But Kane's method had been applied to multibody dynamics only since the 1960s. Therefore, the first reason could be that many researchers thought "all methods for obtaining equations of motion are equivalent, and traditional methods, such as Newton-Euler's or Lagrange's, though less efficient, produce the same results as Kane's does." (Radetsky, 1985) Nevertheless, when one designs a controller to suppress the instability of high-speed railway vehicle systems, it will become important

whether the applied method can quickly generate real-time responses. Kane's method is to a bulldozer what the classical solutions are to shovels. The difference is obviously in the efficiency and in the running time. Kane's method includes different concepts which do not appear in classical methods, such as the use of reference frames in vector components, the optimally chosen generalised speeds, the introduction of partial velocity and partial angular velocity, and the nonholonomic constraint equations. Consequently, Kane's method can efficiently reduce the effort of deriving equations of motion and simplify the final equations given the limited choices of variables it allows.

The second reason could be aroused in learning Kane's method, the beginner needs more time to get familiar with Kane's approach before doing further research. To help beginner to understand Kane's method much more easily, Tu (2016) showed that Kane's equations for a simple nonholonomic system are the first-order form of generalised speeds and proposed an orthogonal criterion to generate efficient equations of motion. In addition, starting from Kane's equations and introducing kinetic energy or acceleration energy functions, he derived four kinds of Lagrange's or Gibbs-Appell's forms of Kane's equations that provide the connection between Kane's method and classical methods.

In the literature, the linearised equations of motion for a wheelset moving along straight rails had been derived in the textbook of Garg and Dukkipati (1984) via Newton-Euler's method in 1984. Following their derivation process, we can find two major drawbacks which make the calculation inefficient and inaccurate. One is the nonlinear equations of motion must be derived first and then those smaller terms be cancelled. However, they had decided to neglect some small terms in the derivation process because of the mathematical complexity. The other is because the equations of motion are in terms of the displacement variable, the contact conditions between wheels and rails must be double checked by the calculated vertical displacement, which should be less than the height of wheel flange (Lee and Cheng, 2005). As stated in the second paragraph, the two drawbacks can be overcome in Kane's method.

When surveying the literature, the author found that no report formulates equations of motion for rail-vehicle dynamic systems via Kane's method. Accordingly, this paper will apply Kane's method to generate the equations of motion for a railway wheelset travelling along a straight track with a constant forward velocity. Following Kane's approach, kinematics analysis and kinetics analysis will be separated into different sections. The kinematics analysis includes six subsections: reference frames, generalised speeds, constraint equations, partial angular velocities and partial velocities, linearisation, and angular and linear accelerations. Similarly, the kinetics analysis consists of generalised active forces and generalised inertia forces. The obtained equations of motion based on Kane's method are compared with those in the literature. At last, the variable parameter of the wheelset system at critical speeds will be investigated.

2 Kinematics analysis

The left and right wheels with conicity angles δ_L and δ_R (Figure 1) are rigidly mounted on a rigid common axle to form a wheelset and these angles are measured between the tangential direction of each contact point and the axial direction

of the wheelset. Research that focused on the lateral motion of the wheelset system typically assumes that the wheelset is moving along straight rails at a constant speed V. The wheelset is also assumed to be kept in close contact with the rails during motion, and the contact points between the wheels and the rails are denoted as P and Q, respectively.

Figure 1 The contact points and unit vectors of the wheelset/rail system (rear view)

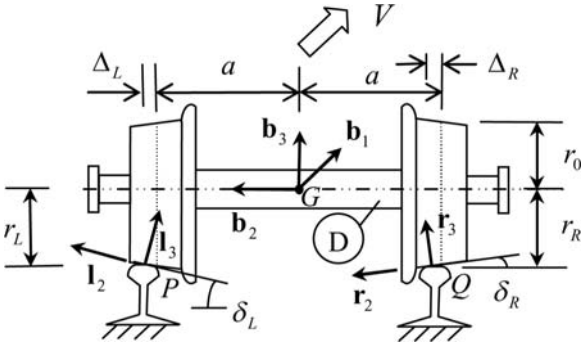

2.1 Reference frames and unit vectors

Two orthogonal unit vector systems, i.e., $\mathbf{n}_i (i = 1, 2, 3)$ and $\mathbf{a}_i (i = 1, 2, 3)$, constitute an inertial reference frame N and an intermediate reference frame A (Figure 2), respectively. The mutually perpendicular unit vector system, $\mathbf{b}_i (i = 1, 2, 3)$, shown in Figure 1 denotes a reference frame B which has its origin at the mass centre G and each aligned with a principal axis of the wheelset. The reference frame A is formed by rotating $\mathbf{n}_i (i = 1, 2, 3)$ anti-clockwise through a yaw angle ψ about unit vector $\mathbf{n}_3$; likewise, the reference frame B is formed by rotating $\mathbf{a}_i (i = 1, 2, 3)$ anticlockwise through a roll angle φ about $\mathbf{a}_1$. Table 1 presents the direction cosines matrices between these two sets of unit vector systems: $\mathbf{n}_i (i = 1, 2, 3)$ and $\mathbf{a}_i (i = 1, 2, 3)$, together with $\mathbf{a}_i (i = 1, 2, 3)$ and $\mathbf{b}_i (i = 1, 2, 3)$, respectively. The relationships between $\mathbf{n}_i (i = 1, 2, 3)$ and $\mathbf{b}_i (i = 1, 2, 3)$ now are

$$\mathbf{n}_1 = \cos\psi\,\mathbf{b}_1 - \sin\psi\,\cos\varphi\,\mathbf{b}_2 + \sin\psi\,\sin\varphi\,\mathbf{b}_3, \tag{1}$$

$$\mathbf{n}_2 = \sin\psi\,\mathbf{b}_1 + \cos\psi\,\cos\varphi\,\mathbf{b}_2 - \cos\psi\,\sin\varphi\,\mathbf{b}_3, \tag{2}$$

$$\mathbf{n}_3 = \sin\varphi\,\mathbf{b}_2 + \cos\varphi\,\mathbf{b}_3 \tag{3}$$

Note that $\mathbf{l}_i (i = 1, 2, 3)$ and $\mathbf{r}_i (i = 1, 2, 3)$ represent the orthogonal unit vectors at P and Q, respectively and Table 2 depicts the direction cosines matrices between $\mathbf{l}_i (i = 1, 2, 3)$ and $\mathbf{b}_i (i = 1, 2, 3)$ along with $\mathbf{r}_i (i = 1, 2, 3)$ and $\mathbf{b}_i (i = 1, 2, 3)$, respectively.

Figure 2 Reference frames and their corresponding unit vectors

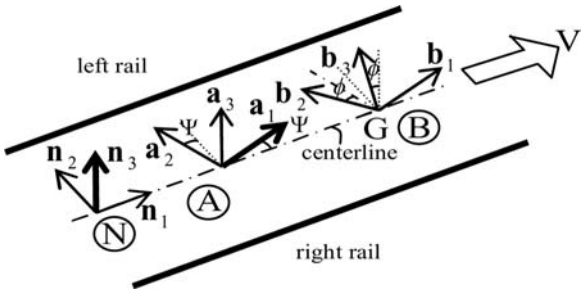

Table 1 The direction cosines matrices of $\mathbf{n}_i(i=1,2,3)$ and $\mathbf{a}_i(i=1,2,3)$ along with of $\mathbf{a}_i(i=1,2,3)$ and $\mathbf{b}_i(i=1,2,3)$

	$\mathbf{n}_1$	$\mathbf{n}_2$	$\mathbf{n}_3$
$\mathbf{a}_1$	$\cos\psi$	$\sin\psi$	0
$\mathbf{a}_2$	$-\sin\psi$	$\cos\psi$	0
$\mathbf{a}_3$	0	0	1

	$\mathbf{a}_1$	$\mathbf{a}_2$	$\mathbf{a}_3$
$\mathbf{b}_1$	1	0	0
$\mathbf{b}_2$	0	$\cos\phi$	$\sin\phi$
$\mathbf{b}_3$	0	$-\sin\phi$	$\cos\phi$

Table 2 The direction cosines matrices of $\mathbf{b}_i(i=1,2,3)$ and $\mathbf{l}_i(i=1,2,3)$ along with of $\mathbf{b}_i(i=1,2,3)$ and $\mathbf{r}_i(i=1,2,3)$

	$\mathbf{b}_1$	$\mathbf{b}_2$	$\mathbf{b}_3$
$\mathbf{l}_1$	1	0	0
$\mathbf{l}_2$	0	$\cos\delta_L$	$\sin\delta_L$
$\mathbf{l}_3$	0	$-\sin\delta_L$	$\cos\delta_L$

	$\mathbf{b}_1$	$\mathbf{b}_2$	$\mathbf{b}_3$
$\mathbf{r}_1$	1	0	0
$\mathbf{r}_2$	0	$\cos\delta_R$	$-\sin\delta_R$
$\mathbf{r}_3$	0	$\sin\delta_R$	$\cos\delta_R$

2.2 Generalised speeds

Assume that another reference frame D is attached to the wheelset (Figure 1). The angle ϕ denotes the forward spinning angle of the wheel and the perturbation angular displacement from a nominal value about $\mathbf{b}_2$ is neglected. Based on the concept of simple angular velocity (Roithmayr and Hodges, 2016), the relative angular velocities between two reference frames of N, A, or A, B, or B, D are

$$^N\boldsymbol{\omega}^A = \dot{\psi}\mathbf{n}_3,\ ^A\boldsymbol{\omega}^B = \dot{\phi}\mathbf{a}_1,\ ^B\boldsymbol{\omega}^D = \dot{\phi}\mathbf{b}_2, \tag{4}$$

where the superscripts on angular velocities stand for the rigid body or the reference frames. Now, if the angular velocity of D with respect to N is taken as

$$^{N}\boldsymbol{\omega}^{D}=u_1\mathbf{b}_1+u_2\mathbf{b}_2+u_3\mathbf{b}_3 \tag{5}$$

and the following auxiliary equation

$$^{N}\boldsymbol{\omega}^{D}=^{N}\boldsymbol{\omega}^{A}+^{A}\boldsymbol{\omega}^{B}+^{B}\boldsymbol{\omega}^{D} \tag{6}$$

is used, then the relationship among generalised speeds $u_i(i=1,2,3)$ and time derivatives of angles ψ, φ, and ϕ are

$$\dot{\psi}=\sec\varphi u_3 \tag{7}$$

$$\dot{\varphi}=u_1 \tag{8}$$

$$\dot{\phi}=u_2-\tan\varphi u_3 \tag{9}$$

Likewise, the velocity of mass centre G of the wheelset is now taken as

$$^{N}\mathbf{v}^{G}=u_4\mathbf{n}_1+u_5\mathbf{n}_2+u_6\mathbf{n}_3,, \tag{10}$$

where the relationships between the generalised speeds $u_i(i=4,5,6)$ and the time derivatives of the coordinates x, y, and z of G are

$$\dot{x}=u_4,\dot{y}=u_5,\dot{z}=u_6. \tag{11}$$

Introducing equations (1)–(3) into equation (10) yields

$$\begin{aligned}^{N}\mathbf{v}^{G}=&(\cos\psi u_4+\sin\psi u_5)\mathbf{b}_1+(-\sin\psi\cos\varphi u_4+\cos\psi\cos\varphi u_5+\sin\varphi u_6)\mathbf{b}_2\\&+(\sin\psi\sin\varphi u_4-\cos\psi\sin\varphi u_5+\cos\varphi u_6)\mathbf{b}_3.\end{aligned} \tag{12}$$

Because an unconstrained wheelset in space has six degrees of freedom, six generalised speeds, $u_i(i=1,2,\ldots,6)$, are thus taken to correspond with. When we consider only the lateral vibration of the constrained wheelset, the wheelset possesses two degrees of freedom. Thus, u_3 and u_5 are kept in the work and the constraint equations on u_1, u_2, u_4, and u_6 in terms of u_3 and u_5 will be found later.

2.3 Constraint equations

When the rigid wheelset is moving forward at a constant speed V, the generalised speed u_4 and the forward spinning angle rate, $\dot{\phi}$, of the wheels of the axle are respectively as

$$u_4=V \tag{13}$$

$$\dot{\phi}=V\big/r_0, \tag{14}$$

where r_0 denotes nominal rolling radius of the wheelset. Substituting equation (14) into equation (9) yields

$$u_2 = \tan\varphi u_3 + V/r_0 . \tag{15}$$

Next, kinematic equations used in the wheelset at contact points P and Q are

$$^N\mathbf{v}^P = {}^N\mathbf{v}^G + {}^N\boldsymbol{\omega}^D \times \mathbf{r}^{P/G} \tag{16}$$

$$^N\mathbf{v}^Q = {}^N\mathbf{v}^G + {}^N\boldsymbol{\omega}^D \times \mathbf{r}^{Q/G} \tag{17}$$

and the position vectors now are

$$\mathbf{r}^{P/G} = (a-\Delta_L)\mathbf{b}_2 - r_L\mathbf{b}_3 , \ \mathbf{r}^{Q/G} = -(a+\Delta_R)\mathbf{b}_2 - r_R\mathbf{b}_3, \tag{18}$$

where Δ_L and Δ_R denote the lateral displacement of contact points from their equilibrium positions. After performing some vector operation, the velocities at contact points P and Q can be expressed as

$$\begin{aligned} ^N\mathbf{v}^P = {} & [-(r_L\tan\varphi + a - \Delta_L)u_3 + \sin\psi\, u_5 + V(\cos\psi - r_L/r_0)]\mathbf{l}_1 \\ & + \{[(a-\Delta_L)\sin\delta_L + r_L\cos\delta_L]u_1 + \sin(\delta_L+\varphi)u_6 + \cos(\delta_L+\varphi)(u_5\cos\psi - V\sin\psi)\}\mathbf{l}_2 \\ & + \{[(a-\Delta_L)\cos\delta_L - r_L\sin\delta_L]u_1 + \cos(\delta_L+\varphi)u_6 - \sin(\delta_L+\varphi)(u_5\cos\psi - V\sin\psi)\}\mathbf{l}_3 \end{aligned} \tag{19}$$

$$\begin{aligned} ^N\mathbf{v}^Q = {} & [-(r_R\tan\varphi - a - \Delta_R)u_3 + \sin\psi\, u_5 + V(\cos\psi - r_R/r_0)]\mathbf{r}_1 \\ & + \{[(a+\Delta_R)\sin\delta_R + r_R\cos\delta_R]u_1 - \sin(\delta_R-\varphi)u_6 + \cos(\delta_R-\varphi)(u_5\cos\psi - V\sin\psi\}\mathbf{r}_2 \\ & + \{-[(a+\Delta_R)\cos\delta_R - r_R\sin\delta_R]u_1 + \cos(\delta_R-\varphi)u_6 + \sin(\delta_R-\varphi)(u_5\cos\psi - V\sin\psi\}\mathbf{r}_3, \end{aligned} \tag{20}$$

where r_L and r_R are written as (Figure 1)

$$r_L = r_0 + y\tan\delta_L \ , \ r_R = r_0 - y\tan\delta_R . \tag{21}$$

The wheels of the wheelset are assumed to be always in contact with the rails, therefore, the velocity components at contact points in their normal directions are zero. That means

$$^N\mathbf{v}^P \cdot \mathbf{l}_3 = 0 \tag{22}$$

$$^N\mathbf{v}^Q \cdot \mathbf{r}_3 = 0. \tag{23}$$

Substituting equations (19) and (20) into equations (22) and (23) yields

$$[(a-\Delta_L)\cos\delta_L - r_L\sin\delta_L]u_1 + \cos(\delta_L+\varphi)u_6 = \sin(\delta_L+\varphi)(u_5\cos\psi - V\sin\psi) \tag{24}$$

$$-[(a+\Delta_R)\cos\delta_R - r_R\sin\delta_R]u_1 + \cos(\delta_R-\varphi)u_6 = -\sin(\delta_R-\varphi)(u_5\cos\psi - V\sin\psi) \tag{25}$$

Solving equations (24) and (25) simultaneously arrives at

$$u_1 = \frac{\Delta_1}{\Delta}(u_5\cos\psi - V\sin\psi) \tag{26}$$

$$u_6 = \frac{\Delta_6}{\Delta}(u_5\cos\psi - V\sin\psi), \tag{27}$$

where Δ, Δ_1, and Δ_6 are

$$\Delta = [(a-\Delta_L)\cos\delta_L - r_L\sin\delta_L]\cos(\delta_R-\varphi)+[(a+\Delta_R)\cos\delta_R - r_R\sin\delta_R]\cos(\delta_L+\varphi) \tag{28}$$

$$\Delta_1 = \sin(\delta_L+\delta_R) \tag{29}$$

$$\Delta_6 = -[(a-\Delta_L)\cos\delta_L - r_L\sin\delta_L]\sin(\delta_R-\varphi)+[(a+\Delta_R)\cos\delta_R - r_R\sin\delta_R]\sin(\delta_L+\varphi). \tag{30}$$

Observation in equations (26) and (27), the roll and vertical velocity of the wheelset/rail system are related to its lateral velocity only. Note that equation (13) is one holonomic constraint equation, while equations (15), (26), and (27) are three nonholonomic constraint equations for the wheelset/rail system.

2.4 Partial angular velocities and partial velocities

The angular velocity of the wheelset *D* with two independent generalised speeds u_3 and u_5 can be expressed as

$${}^N\boldsymbol{\omega}^D = u_3\,{}^N\boldsymbol{\omega}_1^D + u_5\,{}^N\boldsymbol{\omega}_2^D + {}^N\boldsymbol{\omega}_t^D \tag{31}$$

which is developed by Kane (Roithmayr and Hodges, 2016; Kane et al., 1983). With the aid of equations (5), (15), and (26), the partial angular velocities of D are thus

$${}^N\boldsymbol{\omega}_1^D = \tan\varphi\,\mathbf{b}_2 + \mathbf{b}_3 \tag{32}$$

$${}^N\boldsymbol{\omega}_2^D = \frac{\Delta_1\cos\psi}{\Delta}\mathbf{b}_1 \tag{33}$$

$${}^N\boldsymbol{\omega}_t^D = -\frac{\Delta_1}{\Delta}V\sin\psi\,\mathbf{b}_1 + \frac{V}{r_0}\mathbf{b}_2 \tag{34}$$

Similarly, substituting equations (13) and (27) into equation (12) converts the velocity of mass centre G of the wheelset in this form

$${}^N\mathbf{v}^G = u_3^N\mathbf{v}_1^G + u_5^N\mathbf{v}_2^G + {}^N\mathbf{v}_t^G. \tag{35}$$

As a result, the partial velocities in G of D with respect to u_3 and u_5 are

$${}^N\mathbf{v}_1^G = \mathbf{0} \tag{36}$$

$${}^N\mathbf{v}_2^G = \sin\psi\,\mathbf{b}_1 + \cos\psi\left(\cos\varphi + \frac{\Delta_6}{\Delta}\sin\varphi\right)\mathbf{b}_2 + \cos\psi\left(-\sin\varphi + \frac{\Delta_6}{\Delta}\cos\varphi\right)\mathbf{b}_3 \tag{37}$$

$${}^N\mathbf{v}_t^G = V\cos\psi\,\mathbf{b}_1 - V\sin\psi(\cos\psi + \frac{\sin\varphi\Delta_6}{\Delta})\mathbf{b}_2 + V\sin\psi\left(\sin\varphi - \frac{\Delta_6}{\Delta}\cos\varphi\right)\mathbf{b}_3. \tag{38}$$

2.5 Linearisation

In the static equilibrium position, the values of x, y, z and ψ, φ, ϕ are all zeros. When the wheelset is moving at a constant forward speed, these angles ψ and φ are usually assumed to be small. We thus have these relationships: $\cos\psi \approx 1$, $\cos\varphi \approx 1$, $\sin\psi \approx \psi$, $\sin\varphi \approx \varphi$, and $\tan\varphi \approx \varphi$. Besides, both of the conicity angles δ_L and δ_R are assumed to be equal to the same small quantity, λ; likewise, Δ_L and Δ_R are very small and can be neglected. To sum up, we have

$$\Delta = 2a\,,\ \Delta_1 = 2\lambda\,,\ \Delta_6 = 2a\varphi \tag{39}$$

$$u_1 = \frac{\lambda}{a}u_5\,,\ u_2 = \varphi u_3 + V\!\!\diagup\!\!r_0\,,\ u_6 = \varphi u_5 \tag{40}$$

$${}^N\boldsymbol{\omega}_1^D = \varphi\mathbf{b}_2 + \mathbf{b}_3\,,\ {}^N\boldsymbol{\omega}_2^D = \frac{\lambda}{a}\mathbf{b}_1 \tag{41}$$

$${}^N\mathbf{v}_2^G = \psi\mathbf{b}_1 + \mathbf{b}_2 \tag{42}$$

$$r_L = r_0 + \lambda y\,,\ r_R = r_0 - \lambda y. \tag{43}$$

Some terms of two-degree and higher-degree, such as φ^2 or $\lambda^3\varphi y$, and others, are much less than *one* and so are neglected in the perturbation process.

Equations (40) and (43) are substituted into equations (19) and (20), respectively, to facilitate the computation of creep forces and creep moments in Section 3.1:

$${}^N\mathbf{v}^P = (-au_3 - \frac{\lambda y}{r_0}V)\mathbf{l}_1 + [(1+\frac{r_0}{a}\lambda)u_5 - \psi V]\mathbf{l}_2 \tag{44}$$

$${}^N\mathbf{v}^Q = (au_3 + \frac{\lambda y}{r_0}V)\mathbf{r}_1 + [(1+\frac{r_0}{a}\lambda)u_5 - \psi V]\mathbf{r}_2 \tag{45}$$

2.6 Angular and linear accelerations

The angular velocity of the reference frame B in N is

$${}^N\boldsymbol{\omega}^B = {}^N\boldsymbol{\omega}^A + {}^A\boldsymbol{\omega}^B = u_1\mathbf{b}_1 + \varphi u_3\mathbf{b}_2 + u_3\mathbf{b}_3 \tag{46}$$

and substituting equation (40) into equation (46) arrives at

$${}^N\boldsymbol{\omega}^B = \frac{\lambda}{a}u_5\mathbf{b}_1 + \varphi u_3\mathbf{b}_2 + u_3\mathbf{b}_3 \tag{47}$$

Using the following kinematic relationship yields the angular acceleration of wheelset D in N as

$${}^N\boldsymbol{\alpha}^D = \frac{{}^Bd\,{}^N\boldsymbol{\omega}^D}{dt} + {}^N\boldsymbol{\omega}^B \times {}^N\boldsymbol{\omega}^D = \alpha_1\mathbf{b}_1 + \alpha_2\mathbf{b}_2 + \alpha_3\mathbf{b}_3 \tag{48}$$

where $\alpha_i (i = 1, 2, 3)$ are determined as

$$\alpha_1 = \frac{\lambda}{a}\dot{u}_5 - \frac{V}{r_0}u_3,\ \alpha_2 = 0,\ \alpha_3 = \dot{u}_3 + \frac{V\lambda}{r_0\, a}u_5. \tag{49}$$

At the same time, the acceleration of G of the wheelset can be generated by using the kinematic relationship as

$${}^N\mathbf{a}^G = \frac{{}^B d\,{}^N\mathbf{v}^G}{dt} + {}^N\boldsymbol{\omega}^B \times {}^N\mathbf{v}^G = \dot{u}_5\mathbf{b}_2. \tag{50}$$

3 Kinetics analysis

The expressions for generalised active forces and generalised inertia forces are formulated in this section.

3.1 Generalised active forces

According to Kane's method, the constraint forces never contribute to generalised active forces. The active forces in the wheelset/rail system, therefore, contain the creep forces at contact points, the resultant force of the suspension system, and the axle load W_A of the wheelset (including the weight of the wheelset).

3.1.1 Creep forces and creep moments

The wheelset's dynamic behaviour is significantly affected by creep forces and creep moments which arise between the wheels and the rails. Among various wheel-rail rolling contact theories (Garg and Dukkipati, 1984), Kalker's linear creep theory, which has a negligible effect of variation of the normal reaction on the value of the creep coefficients, is applied in this work.

Creep forces and creep moments are remarkably influenced by the area of contact and contact stresses between the wheel and rail and generally defined as functions of creepages on the elliptical contact surface (Figure 3). The definitions of creepages, ξ_1, (ξ_2, ξ_{sp}) are the ratios of the difference between a wheel's longitudinal (transverse, spin) speed and a rail's longitudinal (transverse, spin) speed at the contact point, and the nominal speed V. Based on these definitions, the creepages of the left wheel are

$$\xi_{1L} = ({}^N\mathbf{v}^P \cdot \mathbf{l}_1)/V = -\frac{a}{V}u_3 - \frac{\lambda}{r_0}y \tag{51}$$

$$\xi_{2L} = ({}^N\mathbf{v}^P \cdot \mathbf{l}_2)/V = (1 + \frac{\lambda r_0}{a})\frac{u_5}{V} - \psi \tag{52}$$

$$\xi_{spL} = ({}^N\boldsymbol{\omega}^D \cdot \mathbf{l}_3)/V = \frac{1}{V}u_3 - \frac{\lambda}{r_0}. \tag{53}$$

Figure 3 The wheel/rail contact zone

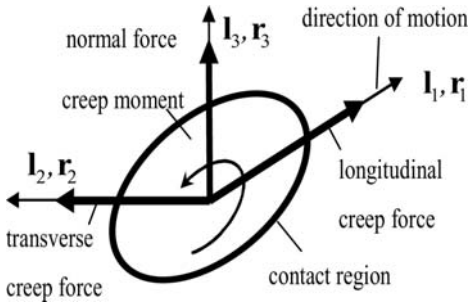

In this case, the creep force $\mathbf{F}_L$ applied to the left wheel is

$$\mathbf{F}_L = -f_{33}\xi_{1L}\mathbf{l}_1 + (-f_{11}\xi_{2L} - f_{12}\xi_{spL})\mathbf{l}_2 \tag{54}$$

and the creep moment $\mathbf{M}_L$ is

$$\mathbf{M}_L = (f_{12}\xi_{2L} - f_{22}\xi_{spL})\mathbf{l}_3 \tag{55}$$

Note that f_{11}, f_{12}, f_{22}, and f_{33} denote lateral, lateral/spin, spin, and longitudinal creep force coefficients, respectively. Likewise, the creepages of the right wheel are

$$\xi_{1R} = ({}^N\mathbf{v}^Q \cdot \mathbf{r}_1)/V = \frac{a}{V}u_3 + \frac{\lambda}{r_0}y \tag{56}$$

$$\xi_{2R} = ({}^N\mathbf{v}^Q \cdot \mathbf{r}_2)/V = (1+\frac{\lambda r_0}{a})\frac{u_5}{V} - \psi \tag{57}$$

$$\xi_{spR} = ({}^N\boldsymbol{\omega}^D \cdot \mathbf{r}_3)/V = \frac{1}{V}u_3 + \frac{\lambda}{r_0} \tag{58}$$

and the creep force $\mathbf{F}_R$ and the creep moment $\mathbf{M}_R$ of the right wheel are

$$\mathbf{F}_R = -f_{33}\xi_{1R}\mathbf{r}_1 + (-f_{11}\xi_{2R} - f_{12}\xi_{spR})\mathbf{r}_2 \tag{59}$$

$$\mathbf{M}_R = (f_{12}\xi_{2R} - f_{22}\xi_{spR})\mathbf{r}_3. \tag{60}$$

To facilitate the subsequent derivation of equations of motion, the relationships of creepages are computed as

$$\xi_{1L} + \xi_{1R} = 0 \tag{61}$$

$$\xi_{1L} - \xi_{1R} = -\frac{2a}{V}u_3 - \frac{2\lambda}{r_0}y \tag{62}$$

$$\xi_{1L}r_L + \xi_{1R}r_R = 0 \tag{63}$$

$$\xi_{2L} + \xi_{2R} = 2\left[\left(1+\frac{\lambda}{a}r_0\right)\frac{u_5}{V} - \psi\right] \tag{64}$$

$$\xi_{2L} r_L + \xi_{2R} r_R = 2r_0 \left[\left(1 + \frac{\lambda}{a} r_0 \right) \frac{u_5}{V} - \psi \right] \tag{65}$$

$$\xi_{spL} + \xi_{spR} = \frac{2}{V} u_3 \tag{66}$$

$$\xi_{spL} r_L + \xi_{spR} r_R = \frac{2r_0}{V} u_3 . \tag{67}$$

3.1.2 Resultant force of suspension system and axle load

As depicted in Figure 4, the resultant force $\mathbf{F}_S$ and the resultant moment $\mathbf{M}_S$ of the suspension systems of the wheelset with a strong truck frame can be expressed as

$$\mathbf{F}_S = -(2k_x x + 2c_x u_4)\mathbf{n}_1 - (2k_y y + 2c_y u_5)\mathbf{n}_2 \tag{68}$$

$$\mathbf{M}_S = -(k_\psi \psi + c_\psi u_3)\mathbf{n}_3 \tag{69}$$

where k_x, c_x and k_y, c_y denote the spring constants and damping coefficients in x- and y-directions, respectively. Now the yaw spring constant k_ψ and yaw damping coefficient c_ψ can be written as

$$k_\psi = 2b^2 k_x , c_\psi = 2b^2 c_x , \tag{70}$$

where b is half length of the spacing between two suspension systems.

Similarly, we consider the axle load applied to the mass centre G of the wheelset as

$$\mathbf{W}_A = -W_A \mathbf{n}_3 \tag{71}$$

Figure 4 The wheelset/rail and suspension system

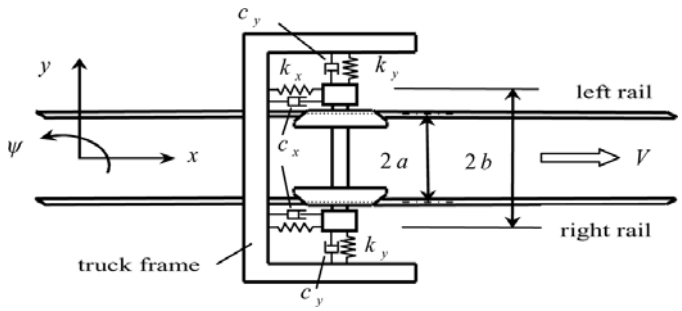

3.1.3 Resultant active force

The resultant active force $\mathbf{R}$ applied to the wheelset now is

$$\begin{aligned} \mathbf{R} &= \mathbf{F}_L + \mathbf{F}_R + \mathbf{F}_S + \mathbf{W}_A \\ &= -(2k_x x + 2c_x u_4)\mathbf{b}_1 - [f_{11}(\xi_{2L} + \xi_{2R}) + f_{12}(\xi_{spL} + \xi_{spR}) + 2k_y y + 2c_y u_5 + W_A \varphi]\mathbf{b}_2 - W_A \mathbf{b}_3 \end{aligned} \tag{72}$$

and the resultant active moment $\mathbf{T}$ about the mass centre G of the wheelset is

$$\begin{aligned}\mathbf{T} &= \mathbf{r}^{P/G}\times\mathbf{F}_L + \mathbf{r}^{Q/G}\times\mathbf{F}_R + \mathbf{M}_L + \mathbf{M}_R + \mathbf{M}_S \\ &= -\{f_{11}(\xi_{2L}r_L + \xi_{2R}r_R) + f_{12}(\xi_{spL}r_L + \xi_{spR}r_R) + a\lambda[f_{11}(\xi_{2L} + \xi_{2R}) + f_{12}(\xi_{spL} + \xi_{spR})]\}\mathbf{b}_1 \\ &\quad + \{-\lambda[f_{12}(\xi_{2L} - \xi_{2R}) - f_{22}(\xi_{spL} - \xi_{spR})]\}\mathbf{b}_2 \\ &\quad + [af_{33}(\xi_{1L} - \xi_{1R}) + f_{12}(\xi_{2L} + \xi_{2R}) - f_{22}(\xi_{spL} + \xi_{spR}) - k_\psi\psi - c_\psi u_3]\mathbf{b}_3\end{aligned} \tag{73}$$

Moreover, the formula for generalised active forces defined by Kane (Roithmayr and Hodges, 2016; Kane et al., 1983) is

$$\tilde{K}_i = {}^N\boldsymbol{\omega}_i^D \cdot \mathbf{T} + {}^N\mathbf{v}_i^G \cdot \mathbf{R} \qquad (i = 1, 2) \tag{74}$$

where ${}^N\boldsymbol{\omega}_i^D (i = 1, 2)$ and ${}^N\mathbf{v}_i^G (i = 1, 2)$ are the partial angular velocities of the wheelset and the partial velocities of G, respectively, which have been derived in equation (31) and equation (35). After performing some mathematical operations, $\tilde{K}_1$ and $\tilde{K}_2$ become

$$\tilde{K}_1 = af_{33}(\xi_{1L} - \xi_{1R}) + f_{12}(\xi_{2L} + \xi_{2R}) - f_{22}(\xi_{spL} + \xi_{spR}) - c_\psi u_3 - k_\psi\psi \tag{75}$$

$$\begin{aligned}\tilde{K}_2 &= -f_{11}\left[\frac{\lambda}{a}(\xi_{2L}r_L + \xi_{2R}r_R) + (\xi_{2L} + \xi_{2R})\right] \\ &\quad - f_{12}\left[\frac{\lambda}{a}(\xi_{spL}r_L + \xi_{spR}r_R) + (\xi_{spL} + \xi_{spR})\right] - 2c_y u_5 - 2k_y y - W_A\varphi\end{aligned} \tag{76}$$

3.2 Generalised inertial forces

When the inertial force and inertial moment about G of the wheelset are obtained, the generalised inertial forces can be calculated. Using equation (50), the inertial force $\mathbf{R}^*$ of G in N is

$$\mathbf{R}^* = -m\,{}^N\mathbf{a}^G = -m\dot{u}_5\mathbf{b}_2 \tag{77}$$

and the resulting inertial moment $\mathbf{T}^*$ with respect to G is

$$\mathbf{T}^* = -[\alpha_1 I_1 - u_2u_3(I_2 - I_3)]\mathbf{b}_1 - [\alpha_2 I_2 - u_3u_1(I_3 - I_1)]\mathbf{b}_2 - [\alpha_3 I_3 - u_1u_2(I_1 - I_2)]\mathbf{b}_3 \tag{78}$$

where $I_i (i = 1, 2, 3)$ stand for the principal mass moments of inertia of the wheelset. Considering the symmetry of the wheelset ($I_3 = I_1$) and noting that $\alpha_2 = 0$, the above equation becomes

$$\mathbf{T}^* = -[\alpha_1 I_1 - u_2u_3(I_2 - I_1)]\mathbf{b}_1 - [\alpha_3 I_1 - u_1u_2(I_1 - I_2)]\mathbf{b}_3. \tag{79}$$

Now, the definition of the generalised inertial forces in Kane's method (Roithmayr and Hodges, 2016; Kane et al., 1983) is

$$\tilde{K}_i^* = {}^N\boldsymbol{\omega}_i^D \cdot \mathbf{T}^* + {}^N\mathbf{v}_i^G \cdot \mathbf{R}^* \qquad (i = 1,\ 2). \tag{80}$$

Substituting the corresponding terms into equation (80), $\tilde{K}_i^* (i = 1,\ 2)$ are computed as follows:

$$\tilde{K}_1^* = -\alpha_3 I_1 + u_1 u_2 (I_1 - I_2) \tag{81}$$

$$\tilde{K}_2^* = -\frac{\lambda}{a}[\alpha_1 I_1 - u_2 u_3 (I_2 - I_1)] - m\dot{u}_5. \tag{82}$$

4 Linearised equations of motion for a wheelset system

4.1 Kane's dynamic equations

When the expressions for generalised active force and generalised inertial force are generated, Kane's dynamic equations for the wheelset system can be expressed as follows:

$$\tilde{K}_i + \tilde{K}_i^* = 0 \qquad (i = 1, 2) \tag{83}$$

It is worth to note that because the partial angular velocities ${}^N\boldsymbol{\omega}_i^D (i = 1, 2)$ and partial velocities ${}^N\mathbf{v}_i^G (i = 1, 2)$ are mutually orthogonal in equation (80), the equations of motion derived below (equation (86) and equation (87)) will be dynamic decoupling (Tu, 2016). That is to say, each equation includes $\dot{u}_3$ or $\dot{u}_5$ only.

Performing some mathematical operations and collecting like terms in equation (83) gives

$$af_{33}(\xi_{1L} - \xi_{1R}) + f_{12}(\xi_{2L} + \xi_{2R}) - f_{22}(\xi_{spL} + \xi_{spR}) - c_\psi u_3 - k_\psi \psi - \alpha_3 I_1 + u_1 u_2 (I_1 - I_2) = 0 \tag{84}$$

$$-f_{11}[\frac{\lambda}{a}(\xi_{2L} r_L + \xi_{2R} r_R) + (\xi_{2L} + \xi_{2R})] - f_{12}[\frac{\lambda}{a}(\xi_{spL} r_L + \xi_{spR} r_R) + (\xi_{spL} + \xi_{spR})]$$

$$-2c_y u_5 - 2k_y y - W_A \varphi - \frac{\lambda}{a}[\alpha_1 I_1 - u_2 u_3 (I_2 - I_1)] - m\dot{u}_5 = 0 \tag{85}$$

Substituting equations (61)–(67) into equations (84) and equation (85) and ignoring small terms yield

$$I_1 \dot{u}_3 = -\left[\frac{2}{V}(f_{22} + a^2 f_{33}) + c_\psi\right] u_3 + \left[\frac{2 f_{12}}{V}(1 + \frac{\lambda}{a} r_0) - \frac{\lambda I_2}{a r_0} V\right] u_5 - (2 f_{12} + k_\psi)\psi - \frac{2\lambda a}{r_0} f_{33} y \tag{86}$$

$$m\dot{u}_5 = -\left[\frac{2 f_{12}}{V}(1 + \frac{\lambda}{a} r_0) - \frac{\lambda I_2}{a r_0} V\right] u_3 - \left[\frac{2 f_{11}}{V}(1 + \frac{\lambda}{a} r_0) + 2c_y\right] u_5 + 2 f_{11}(1 + \frac{\lambda}{a} r_0)\psi - 2k_y y - W_A \varphi \tag{87}$$

In addition, combining equation (8), the second part of equation (11) along with the first part of equation (40), one will get

$$\dot{\varphi} = \frac{\lambda}{a}\dot{y}. \tag{88}$$

Integrating equation (88) and considering zero initial values yields

$$\varphi = \frac{\lambda}{a} y. \tag{89}$$

Substituting equation (89) back to equation (87) yields

$$\begin{aligned} m\dot{u}_5 = &-\left[\frac{2f_{12}}{V}(1+\frac{\lambda}{a}r_0) - \frac{\lambda I_2}{a r_0}V\right]u_3 - \left[\frac{2f_{11}}{V}(1+\frac{\lambda}{a}r_0) + 2c_y\right]u_5 \\ &+ 2f_{11}(1+\frac{\lambda}{a}r_0)\psi - (2k_y + \frac{\lambda}{a}W_A)y. \end{aligned} \tag{90}$$

For later convenience, equations (86) and (90) will be rewritten as

$$I_1\ddot{\psi} + \left[\frac{2}{V}(f_{22}+a^2 f_{33}) + c_\psi\right]\dot{\psi} - \left[\frac{2f_{12}}{V}(1+\frac{\lambda}{a}r_0) - \frac{\lambda I_2}{a r_0}V\right]\dot{y} + (2f_{12}+k_\psi)\psi + \frac{2\lambda a}{r_0} f_{33} y = 0 \tag{91}$$

$$m\ddot{y} + \left[\frac{2f_{12}}{V}(1+\frac{\lambda}{a}r_0) - \frac{\lambda I_2}{a r_0}V\right]\dot{\psi} + \left[\frac{2f_{11}}{V}(1+\frac{\lambda}{a}r_0) + 2c_y\right]\dot{y} - 2f_{11}(1+\frac{\lambda}{a}r_0)\psi + (2k_y + \frac{\lambda}{a}W_A)y = 0 \tag{92}$$

4.2 State equations

Kane's dynamic equations for the wheelset, equations (91) and (92), can be converted into the following state equation.

$$\begin{bmatrix} I_1 & 0 \\ 0 & m \end{bmatrix}\begin{Bmatrix} \ddot{\psi} \\ \ddot{y} \end{Bmatrix} + \begin{bmatrix} \frac{2}{V}(f_{22}+a^2 f_{33}) + c_\psi & -\frac{2f_{12}}{V}(1+\frac{\lambda}{a}r_0) + \frac{\lambda V}{a r_0}I_2 \\ \frac{2f_{12}}{V}(1+\frac{\lambda}{a}r_0) - \frac{\lambda V}{a r_0}I_2 & \frac{2f_{11}}{V}(1+\frac{\lambda}{a}r_0) + 2c_y \end{bmatrix}\begin{Bmatrix} \dot{\psi} \\ \dot{y} \end{Bmatrix} + \begin{bmatrix} 2f_{12}+k_\psi & \frac{2\lambda a}{r_0} f_{33} \\ -2f_{11}(1+\frac{\lambda}{a}r_0) & 2k_y + \frac{\lambda}{a}W_A \end{bmatrix}\begin{Bmatrix} \psi \\ y \end{Bmatrix} = \begin{Bmatrix} 0 \\ 0 \end{Bmatrix} \tag{93}$$

Since no forcing terms are found in equation (93), the wheelset system denotes a damped free vibration system. The damping effect arises from three aspects: creep force, suspension system, and the gyroscopic effect of the wheelset. If we define the spinning damping coefficient c_{sp} as

$$c_{sp} = -\left[\frac{2f_{12}}{V}(1+\frac{\lambda}{a}r_0) - \frac{\lambda I_2}{a r_0}V\right] \tag{94}$$

then the damping matrix in equation (93) can be written as

$$\begin{bmatrix} \frac{2}{V}(f_{22}+a^2 f_{33}) + c_\psi & c_{sp} \\ -c_{sp} & \frac{2f_{11}}{V}(1+\frac{\lambda}{a}r_0) + 2c_y \end{bmatrix} \tag{95}$$

Because the non-diagonal elements in equation (95) are opposite, the wheelset system always possesses a negative damping force either in y or in ψ directions. This might lead the system to be dynamically unstable. A small disturbance could be getting the

vibration of ever-increasing amplitude throughout the range for which these equations of motion are valid. Moreover, f_{11} causes a negative stiffness force while f_{12} might cause a negative damping force as shown in equation (93).

When the generalised speeds $\dot{\psi}$ (or u_3) and $\dot{y}$ (or u_5) were determined from equation (93) with a given set of initial conditions, $\dot{\psi}(0)$, $\dot{y}(0)$, $\psi(0)$, and $y(0)$, the coordinates ψ and y can be determined by integrating equation (93). Similarly, combining Equations (11) and (13) with the third part of equation (40) in matrix form yields

$$\begin{Bmatrix} \dot{x} \\ \dot{y} \\ \dot{z} \end{Bmatrix} = \begin{bmatrix} 0 & 0 \\ 0 & 1 \\ 0 & \varphi \end{bmatrix} \begin{Bmatrix} \dot{\psi} \\ \dot{y} \end{Bmatrix} + \begin{Bmatrix} V \\ 0 \\ 0 \end{Bmatrix}. \tag{96}$$

When generalised speeds $\dot{\psi}$ and $\dot{y}$ were given, coordinates x, y and z can be determined by integrating equation (96) with the specified initial conditions, $x(0)$, $y(0)$, and $z(0)$.

4.3 Comparison with literature

For comparison, the equations of motion of the wheelset in matrix form, derived from the textbook of Garg and Dukkipati (1984), are shown below:

$$\begin{bmatrix} I_1 & 0 \\ 0 & m \end{bmatrix} \begin{Bmatrix} \ddot{\psi} \\ \ddot{y} \end{Bmatrix} + \begin{bmatrix} \frac{2}{V}(f_{22}+a^2 f_{33})+c_\psi & -\frac{2f_{12}}{V}(1+\frac{\lambda}{a}r_0)+\frac{\lambda V}{a\, r_0}I_2 \\ \frac{2f_{12}}{V} & \frac{2f_{11}}{V}(1+\frac{\lambda}{a}r_0)+2c_y \end{bmatrix} \begin{Bmatrix} \dot{\psi} \\ \dot{y} \end{Bmatrix} + \begin{Bmatrix} 2f_{12}+a\lambda W_A+k_\psi & \frac{2\lambda a}{r_0}f_{33} \\ -2f_{11} & 2k_y+\frac{\lambda}{a}W_A \end{Bmatrix} \begin{Bmatrix} \psi \\ y \end{Bmatrix} = \begin{Bmatrix} 0 \\ 0 \end{Bmatrix} \tag{97}$$

The above equation derived via Newton-Euler's method mainly differs from that obtained by Kane's method in two aspects. One is zero yaw gravitational stiffness found in this work and the other one is a gyroscopic effect term neglected in Garg and Dukkipati (1984). The equations of Wagner (2009) and Knudsen et al. (1991) for a wheelset system also include two gyroscopic effect terms but their equations do not consider gravitational stiffness terms.

4.3.1 Lateral and yaw gravitational stiffness

After considering the force equilibrium for the wheelset/rail system, we have

$$\mathbf{F}_L + \mathbf{F}_R + \mathbf{F}_S + \mathbf{W}_A + \mathbf{N}_L + \mathbf{N}_R - m\dot{u}_5\mathbf{b}_2 = \mathbf{0} \tag{98}$$

where the normal reactions $\mathbf{N}_L$ and $\mathbf{N}_R$ at contact points are defined as

$$\mathbf{N}_L = N_L\mathbf{l}_3;\ \mathbf{N}_R = N_R\mathbf{r}_3. \tag{99}$$

When we dot the equation (98) with $\mathbf{r}_2$, we can arrive at

$$N_L = -\frac{1}{2\lambda}[m\dot{u}_5 + f_{11}(\xi_{2L}+\xi_{2R}) + f_{12}(\xi_{spL}+\xi_{spR}) + k_y y + c_y u_5 + W_A(\varphi-\lambda)] \tag{100}$$

Likewise, dotting the equation (98) with $\mathbf{l}_2$ will yield

$$N_R = \frac{1}{2\lambda}[m\dot{u}_5 + f_{11}(\xi_{2L} + \xi_{2R}) + f_{12}(\xi_{spL} + \xi_{spR}) + k_y y + c_y u_5 + W_A(\varphi + \lambda)]. \tag{101}$$

Now, the lateral gravitational stiffness F_g is defined as

$$F_g = (\mathbf{N}_L + \mathbf{N}_R)\cdot\mathbf{n}_2 = -W_A\varphi = -\frac{\lambda}{a}W_A y. \tag{102}$$

From this equation, F_g denotes a restoring force that can bring the wheelset return to the equilibrium position. At the same time, the yaw gravitational stiffness M_g is evaluated as

$$M_g = (\mathbf{r}^{P/G}\times\mathbf{N}_L + \mathbf{r}^{Q/G}\times\mathbf{N}_R)\cdot\mathbf{n}_3 = 0. \tag{103}$$

The zero value of M_g denotes the restoring moment is not required as the wheelset is moving along the tangential rails.

4.3.2 Gyroscopic effect

In general, the wheelset spins at a higher rate than the truck's angular velocity about its axis of symmetry, so the gyroscopic effect (Hibbeler, 1992) occurs. In the situation, the gyroscopic force vector Γ is defined as

$$\mathbf{\Gamma} = {}^N\boldsymbol{\omega}^D \times (I_2\dot{\phi}\mathbf{b}_2) = -I_2\dot{\phi}u_3\mathbf{b}_1 + I_2\dot{\phi}u_1\mathbf{b}_3. \tag{104}$$

An inner product Γ with ${}^N\omega_i^D (i = 1, 2)$ will yield

$${}^N\boldsymbol{\omega}_1^D\cdot\mathbf{\Gamma} = I_2\dot{\phi}u_1,\ {}^N\boldsymbol{\omega}_2^D\cdot\mathbf{\Gamma} = -\frac{\lambda}{a}I_2\dot{\phi}u_3. \tag{105}$$

Consequently, the gyroscopic force appeared in equation (92) is correct.

5 Numerical analysis

To compare the equations of motion of the wheelset in this work with those of Garg and Dukkipati (1984), the parameter values of the wheelset system are taken from Ahmadian and Yang (1998):

$a = 0.7176$ m, $b = 1.0$ m, $r_0 = 0.533$ m, $\lambda = 0.05$, $m = 1800$ kg

$f_{11} = 6.728\times10^6$ N, $f_{22} = 1000$ N-m^2, $f_{12} = 1200$ N-m,

$f_{33} = 6.728\times10^6 N$, $I_1 = 625.7$ kg-m^2, $I_2 = 133.92$kg-m^2,

$k_x = k_y = 8.67\times10^4$ N/m, $c_x = c_y = 2.1\times10^4$ N·s/m.

Because the axle load includes both the weight of the wheelset and another loading from the truck, here $W_A = 38492.4\ N$ is taken.

The only equilibrium point of the considered wheel/rail system is the position $\psi = y = 0$. This critical speed (V_{cr}) can be determined by setting zero Routh's discriminant (Wickens, 1965); thus the critical speeds computed in present analysis and in Garg and Dukkipati (1984) are 164.5 km/hr and 166.9 km/hr, respectively. The

following numerical results show that the results obtained by Garg and Dukkipati (1984) are always overestimated as compared with those computed in this work.

Figure 5(a) and (b) show the variation of critical speeds of the wheelset with respect to conicity angle λ and transverse stiffness k_y, respectively. We found that the larger λ the smaller V_{cr}; on the contrary, the larger k_y the larger V_{cr}. Moreover, since f_{11} will cause a negative stiffness force while f_{12} might cause a negative damping force, Figures 6(a) and 6(b) depict the variety of critical speeds of the wheelset with respect to lateral and lateral/spin creep coefficients, respectively. We found that as f_{11} increases, V_{cr} is from the largest down to the smallest and then reversing from the bottom to increase, as shown in Figure 6(a). By contrast, Figure 6(b) demonstrated that f_{12} has a negligible effect on the critical speeds.

Figure 5 Variation of critical speeds of Garg and Dukkipati (1984) and this work: (a) with conicity angle λ and (b) with transverse stiffness k_y

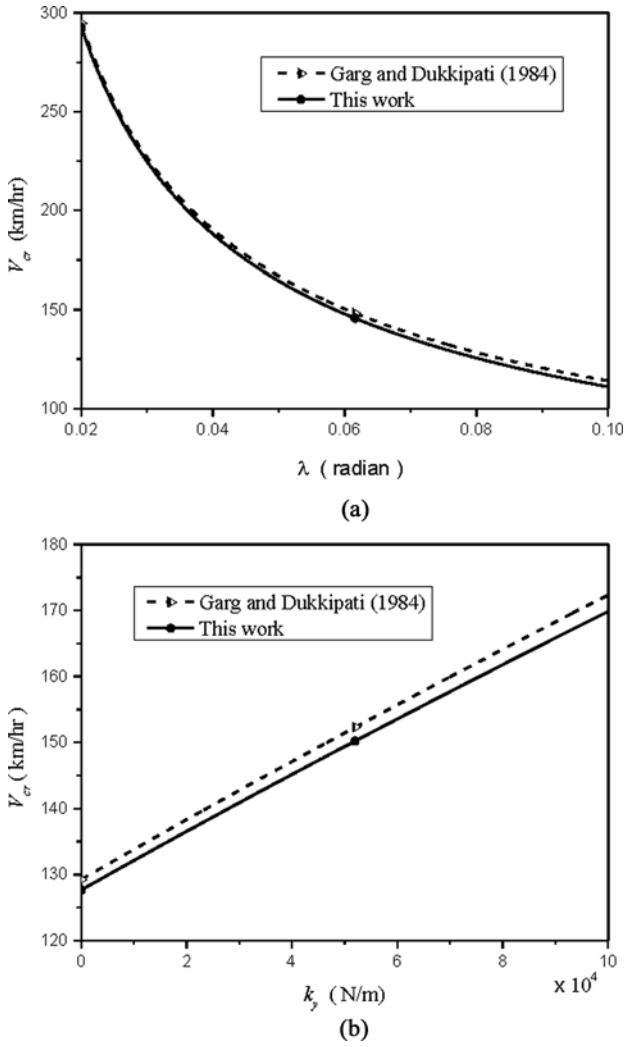

Figure 6 Variation of critical speeds of Garg and Dukkipati (1984) and this work: (a) with f_{11} and (b) with f_{12}

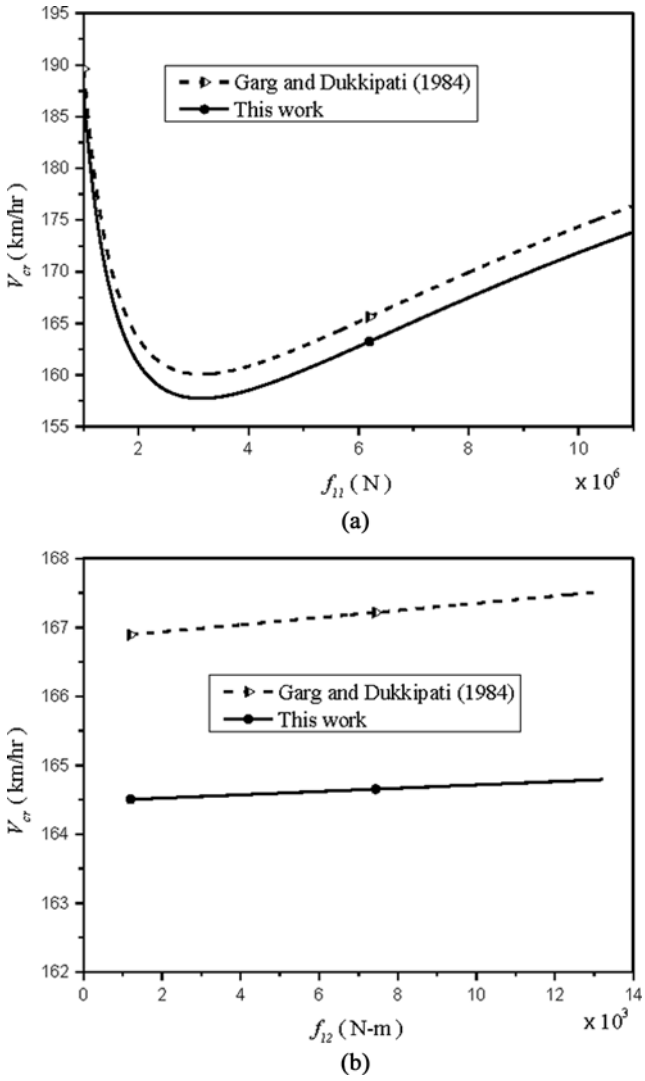

Figures 7(a) and 7(b) illustrate the variation of critical speeds of the wheelset with respect to I_2 and axle load W_A, respectively. We found that the critical speeds increase with respect to I_2 or W_A irrespective of using the equations of Garg and Dukkipati (1984) or of this work. Also, from this figure, we found that V_{cr} of this work is higher than that of Garg and Dukkipati (1984) as I_2 increases to about three times of I_2. The similar result is found in Figure 7(b), but the increment in V_{cr} is finite.

Figure 7 Variation of critical speeds of Garg and Dukkipati (1984) and this work: (a) with I_2 and (b) with W_A

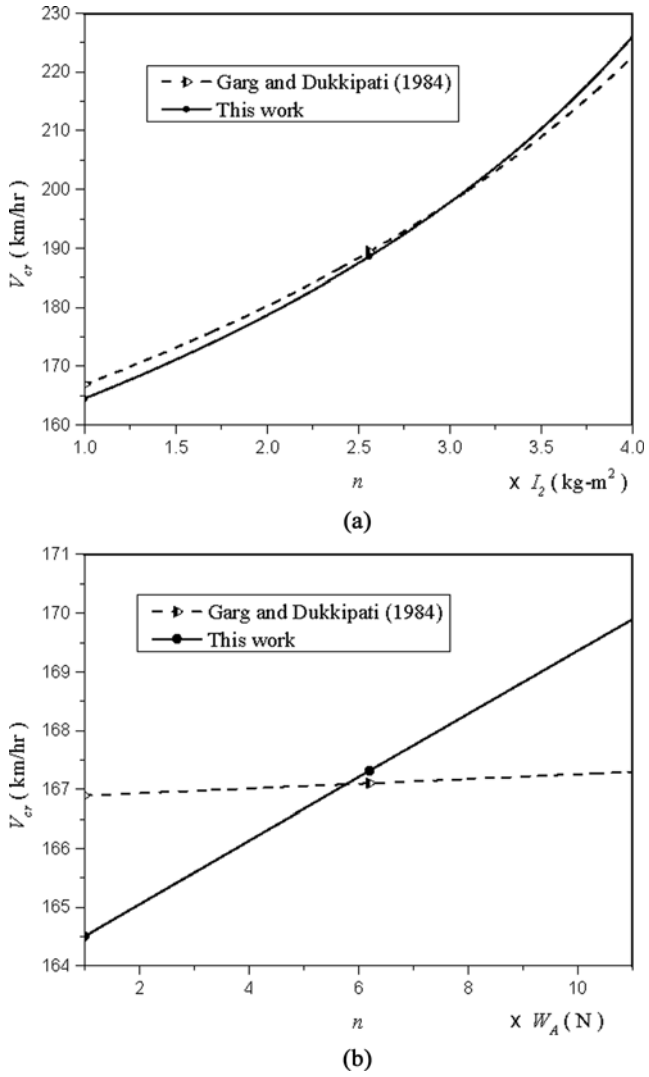

6 Discussions

As depicted above, we have generated the two equations of motion for a railway wheelset travelling on tangential rails by Kane's method. Below, four separated points, the contact conditions between wheels and rails, the dynamic decoupling conditions, the linearisation procedure of Kane's method, and the comparison between Kane's equations and Newton-Euler equations, will be discussed.

6.1 The contact conditions between wheels and rails

Because the wheels of the wheelset are assumed to be always in contact with the rails, Lee and Cheng (2005) computed the vertical displacement of the wheel to assure that its value is less than the height of the wheel flange by using the Newton-Euler method. However, this paper can directly use the motion constraints, that is to say, the velocity components at contact points in their normal directions are zero, without computing the vertical displacement.

In addition, because the definitions of creepages are the ratios of the difference between a wheel's and a rail's speed in various directions, these creepages can directly correspond to generalised speeds. This reflects Kane's method is concerned with motions, not configurations.

6.2 The dynamic decoupling conditions

From the study (Tu, 2016) on promoting Kane's method, one can generate the first-order decoupling equations of motion, as long as the orthogonal conditions of partial velocities are satisfied. Since the two partial angular velocities in equations (32) and (33) are orthogonal to each other and the same as two partial velocities in equation (36) and (37), we can predict the final equations of motion in this work with dynamic decoupling.

Now, if we choose the alternative generalised speeds of angular velocity as follows:

$$^{N}\boldsymbol{\omega}^{D} = u_1 \mathbf{n}_3 + u_2 \mathbf{a}_1 + u_3 \mathbf{b}_2. \tag{106}$$

Namely, the generalised speeds are

$$u_1 = \dot{\psi}, u_2 = \dot{\varphi}, u_3 = \dot{\phi}. \tag{107}$$

Following the same derivation process, we can finally obtain the alternative partial angular velocities as

$$^{N}\boldsymbol{\omega}_1^{D} = \sin\varphi \mathbf{b}_2 + \cos\varphi \mathbf{b}_3,\ ^{N}\boldsymbol{\omega}_2^{D} = \frac{\Delta_1}{\Delta}\cos\psi \mathbf{b}_1. \tag{108}$$

It is apparent that $^{N}\boldsymbol{\omega}_1^{D}$ and $^{N}\boldsymbol{\omega}_2^{D}$ are mutually orthogonal, making the final equations of motion still have the characteristic of dynamic decoupling. The reason is that the roll and vertical velocities of the wheelset/rail system are related to its lateral velocity but are independent of yaw velocity.

6.3 The linearisation procedure of Kane's method

The linearisation methods of equations of motion mainly include post linearisation and kinematics linearisation. The procedure of post linearisation is to derive the fully nonlinear equations of motion first and then linearise these equations. This method is severe and requires more labour. Garg and Dukkipati's equations (Garg and Dukkipati, 1984) are an example. They took Newton-Euler's method to generate the linearised equations of motion for the wheelset/rail system.

On the contrary, Kane's method (Roithmayr and Hodges, 2016; Kane et al., 1983) is an example of the kinematics linearisation method. Kane's method is to develop fully

nonlinear expressions for angular velocity and velocity of the mass centre of the wheelset, then to determine partial angular velocities and partial velocities by inspection. Next, linearise all angular velocities, velocities, partial angular velocities, and partial velocities, and use the linear forms to construct generalised active forces and generalised inertia forces. At the same time, all terms of second or higher degree are discarded. Taking a close look at Kane's method, it can bypass the full nonlinear equations to generate the linearised equations.

6.4 The comparison between Kane's equations and Newton-Euler equations

The final equations of motion derived from Kane's methods are always in the first-order form. Equations (86), (87), and (96) provide the five first-order equations for the wheelset system. When the initial conditions are assigned, one can solve five variables: u_3, u_5, x, y, and z.

On the other hand, the resulting equations of motion generated from Newton-Euler equations are still with second-order form, like equation (97) shown. In numerical analysis, one usually lets

$$y_1 = \dot{\psi},\ y_2 = \dot{y} \tag{109}$$

to transform the original equations to the first-order form, and then numerically finds the solution. Because the generalised speeds u_3 and u_5 in this work are usually the linear combination of time derivatives of generalised coordinates, Kane's equations can obtain the most efficient form in computer implementation.

7 Conclusion

This study has applied Kane's method to derive for the first time the equations of motion of a wheelset that is moving along tangent rails at a constant speed V. Since Kane's method can exactly model the wheel/rail contact conditions to obtain the nonholonomic constraint equations, the wheelset system with lateral vibration is considered a simple nonholonomic system possessing two degrees of freedom. Kane's method can directly be utilised to linearise the equations of motion without first writing exact dynamic equations of motion, and markedly simplify the derivation of equations of motion in stability analysis or in designing a control system. In addition, this work found that two gyroscopic effect terms exist and no yaw gravitational stiffness appears in the equations of motion. Last but not least, the advantage of Kane's method is exactly modelling the contact conditions between wheels and rails by generalised speeds; the derivation procedure of Kane's method is simpler and more systematic than Newton-Euler's or Lagrange's.

Acknowledgement

The author would like to thank the National Science Council of the Republic of China for financially supporting this research under the Contract No. NSC-89-2212-E-344-002.

References

Ahmadian, M. and Yang, S. (1998) "Hopf bifurcation and hunting in a rail wheelset with flange contact", *Nonlinear Dynamics*, Vol. 15, pp.15–30.

Banerjee, A.K. (2016) *Flexible Multibody Dynamics: Efficient Formulations and Applications*, John Wiley & Sons Ltd, West Sussex.

Garg, V.K. and Dukkipati, R.V. (1984) *Dynamics of Railway Vehicles Systems*, Academic Press, London.

Hibbeler, R.C. (1992) *Engineering Mechanics – Dynamics*, 6th ed., Macmillan Publishing Company, New York, pp.511, 512.

Huston, R.L. (1990) *Multibody Dynamics*, Butterworth-Heinemann, Stoneham.

Iwnicki, S. (2006) *Handbook of Railway Vehicle Dynamics*, CRC Press, Taylor & Francis Group, London.

Kane, T.R., Likins, P.W. and Levinson, D.A. (1983) *Spacecraft Dynamics*, McGraw-Hill Book Co., New York.

Knudsen, C., Feldberg, R. and Jaschinski, A. (1991) 'Nonlinear dynamic phenomena in the behaviour of a railway wheelset model', *Nonlinear Dynamics*, Vol. 2, No. 5, pp.389–404.

Lee, S.Y. and Cheng, Y.C. (2005) 'Hunting stability analysis of high-speed railway vehicle trucks on tangent tracks', *Journal of Sound and Vibration*, Vol. 282, pp.881–898.

Radetsky, P. (1985) 'The man who mastered motion', *Science*, Vol. 86, pp.52–60.

Roithmayr, C.M. and Hodges, D.H. (2016) *Dynamics: Theory and Application of Kane's Method*, Cambridge University Press, New York.

Shabana, A.A., Zaazaa, K.E. and Sugiyama, H. (2007) *Railroad Vehicle Dynamics: A Computational Approach*, CRC Press, Taylor & Francis Group, London.

Tu, T.W. (2016) 'First-order form, Lagrange's form, and Gibbs–Appell's form of Kane's equations', *Acta Mechanica*, Vol. 227, No. 7, pp.1885–1901.

Wagner, U.V. (2009) 'Nonlinear dynamic behaviour of a railway wheelset', *Vehicle System Dynamics*, Vol. 47, No. 5, pp.627–640.

Wickens, A.H. (1965) 'The dynamic stability of railway vehicle wheelsets and bogies having profiled wheels', *Int. J. Solids Structures*, Vol. 1, pp.319–341.

Wickens, A.H. (2003) *Fundamentals of Rail Vehicle Dynamics*, CRC Press, Swets & Zeitlinger, Netherlands.

Zhai, W.M. (2015) *Vehicle-Track Coupling Dynamics* (I), 4th ed., Science Publishing, Peking (In Chinese).

Nomenclature

Scalar	
a	Half-length of the track gauge
b	Half-length of the spacing between two suspension systems
A, B	Two reference frames
c_{sp}, c_x, c_y, c_ψ	Spinning, longitudinal, lateral and yaw damping coefficients
D	Reference frame attached in wheelset
$f_{11}, f_{12}, f_{22}, f_{33}$	Lateral, lateral/spin, spin, and longitudinal creep force coefficients
F_g	A restoring force of the wheelset/rail system

G	Mass centre of wheelset
$I_i (i = 1,2,3)$	Roll, spin, and yaw principal mass moments of inertia of wheelset
k_x, k_y, k_ψ	Longitudinal, lateral, and yaw stiffnesses
$\tilde{K}_i, \tilde{K}_i^* (i = 1,2)$	Generalised active forces and generalised inertia forces
m	Mass of wheelset
M_g	A restoring moment of the wheelset/rail system
N	Newtonian reference frame
N_L, N_R	Normal loads at left and right wheels/rails
P, Q	Contact points at left and right wheels/rails
r_0	Nominal rolling radius of wheelset (i.e., radius of wheelset prior to offset)
r_L, r_R	Instantaneous rolling radii of left and right wheels
$u_i (i = 1,\ldots,6)$	Generalised speeds
V	Constant forward speed of wheelset
W_A	Axle load (including the weight of wheelset)
x, y, z	Longitudinal, lateral, and vertical displacements of wheelset mass centre
y_1, y_2	Two variables used in equation (109)
Vector	
${}^N\mathbf{a}^G$	Acceleration of mass centre of wheelset
$\mathbf{a}_i (i = 1,2,3)$	Unit vectors in reference frame A
$\mathbf{b}_i (i = 1,2,3)$	Unit vectors in reference frame B
$\mathbf{F}_L, \mathbf{F}_R$	Linear creep forces of left and right wheels
$\mathbf{F}_S$	Force vector of suspension system
$\mathbf{l}_i (i = 1,2,3)$	Unit vectors at contact point P
$\mathbf{M}_L, \mathbf{M}_R$	Linear creep moments of left and right wheels
$\mathbf{M}_S$	Moment vector of suspension system
$\mathbf{N}_L, \mathbf{N}_R$	Normal reaction vectors at left and right wheels/rails
$\mathbf{n}_i (i = 1,2,3)$	Unit vectors in N
$\mathbf{r}^{P/G}, \mathbf{r}^{Q/G}$	Position vectors
$\mathbf{r}_i (i = 1,2,3)$	Unit vectors at contact point Q
$\mathbf{R}, \mathbf{R}^*$	Total resultant active force and inertia force vectors
$\mathbf{T}, \mathbf{T}^*$	Total resultant active moment and inertia moment vectors due to active forces and inertial forces

${}^N\mathbf{v}^G$, ${}^N\mathbf{v}^P$, ${}^N\mathbf{v}^Q$	velocities of the mass centre and contact points P, Q of wheelset
${}^N\mathbf{v}_1^G$, ${}^N\mathbf{v}_2^G$, ${}^N\mathbf{v}_t^G$	partial velocities of mass centre of wheelset in an inertia reference frame
$\mathbf{W}_A$	Axle load vector applied to the mass centre of wheelset
Greek symbols	
$\alpha_i (i = 1,2,3)$	$\mathbf{b}_i (i = 1,2,3)$ measure numbers of ${}^N\boldsymbol{\alpha}^D$
${}^N\boldsymbol{\alpha}^D$	Angular acceleration of wheelset
δ_L, δ_R	Left and right contact angles
$\Delta, \Delta_1, \Delta_6$	Abbreviations for mathematical expression
Δ_L, Δ_R	Lateral displacements of left and right contact points from their equilibrium positions
φ	Roll angle of wheelset
ϕ	Spinning angle of wheelset
$\boldsymbol{\Gamma}$	Gyroscopic effect term
λ	Wheel conicity angle
${}^N\boldsymbol{\omega}^A$, ${}^A\boldsymbol{\omega}^B$, ${}^B\boldsymbol{\omega}^D$, ${}^N\boldsymbol{\omega}^B$, ${}^N\boldsymbol{\omega}^D$	Several angular velocities used in the derivation process
${}^N\boldsymbol{\omega}_i^D (i = 1,2)$, ${}^N\boldsymbol{\omega}_t^D$	Partial angular velocities of mass centre of wheelset in an inertial reference frame
ξ_1, ξ_2, ξ_{sp}	Longitudinal, transverse, and spin creepages
ψ	Yaw angle of wheelset
Subscripts	
$0,1,2,3,4,5,6, A, g, i,$ $L, R, S, sp, t, x, y, \psi$	Indices
Superscripts	
$A, B, D, G, N, P, Q, *, \sim$	Indices